Regime-Switching Neural-Operator Digital Twins for Gas-Liquid Two-Phase Flow with Bayesian Assimilation and Robust Control Interfaces

Andrés Felipe Montoya[1], **Camilo Andrés Pineda**[2], **and Julián David Restrepo**[3]
[1]Universidad de Nariño, Calle 18 50–02, Ciudadela Torobajo, Pasto, Nariño, Colombia
[2]Universidad del Magdalena, Carrera 32 22–08, Sector San Pedro Alejandrino, Santa Marta, Magdalena, Colombia
[3]Universidad del Quindío, Carrera 15 12N–20, Barrio La Castellana, Armenia, Quindío, Colombia

ABSTRACT Gas–liquid two-phase flow arises across drilling, well control, and pipeline transport, where rapid changes in holdup, pressure gradient, and interfacial structure can trigger operational risk. Although mechanistic models encode conservation laws, their closure relations and regime transitions are often uncertain under field variability, sensor sparsity, and geometry-dependent flow pattern shifts. This paper develops a real-time digital-twin framework that couples a regime-switching state-space model with physics-constrained neural operators to support inference and control under uncertainty. The core contribution is a hybrid architecture in which latent flow regimes act as discrete modes that gate continuous dynamics and closure surrogates, while a neural operator learns nonlocal constitutive mappings consistent with mass and momentum balances. A Bayesian assimilation layer performs joint filtering of continuous states and regime probabilities using likelihood models tailored to typical downhole and topside measurements. The resulting twin yields calibrated predictive distributions rather than point forecasts, enabling robust decision interfaces for choke and pump commands. We provide identifiability conditions for separating regime-induced dynamics from closure uncertainty, derive stability constraints for mode transitions, and present a computational study showing improved predictive reliability under sensor dropout and distribution shift relative to purely data-driven or purely mechanistic baselines. The framework is designed to integrate heterogeneous datasets, including flow-loop experiments and operational telemetry, and it supports online adaptation while maintaining physical consistency through constrained residual minimization.

KEYWORDS

1. Introduction

Operational systems that transport mixtures of gas and liquid are governed by coupled conservation laws, interfacial momentum exchange, and strongly geometry-dependent flow structures [1]. In practice, engineers interact with these systems through sparse sensors, delayed observations, and control actuators that can induce abrupt changes in pressure and phase distribution. A central difficulty is that the macroscopic state variables that matter for safety and economics, such as liquid holdup, pressure gradient, and gas fraction, are shaped by mesoscale structures that reorganize rapidly. These reorganizations are commonly described as flow regimes, but regime labels are only a proxy for a broader set of dynamical modes that alter friction, slip, entrainment, and effective compressibility. As a result, two identical boundary conditions can lead to different transient responses depending on the current internal configuration, which

Article info:
Andrés Felipe Montoya, Camilo Andrés Pineda, and Julián David Restrepo. *Regime-Switching Neural-Operator Digital Twins for Gas-Liquid Two-Phase Flow with Bayesian Assimilation and Robust Control Interfaces.* Grovesocieties . Licensed under Attribution - NonCommercial - No Derivatives 4.0 International (CC BY-NC-ND 4.0)

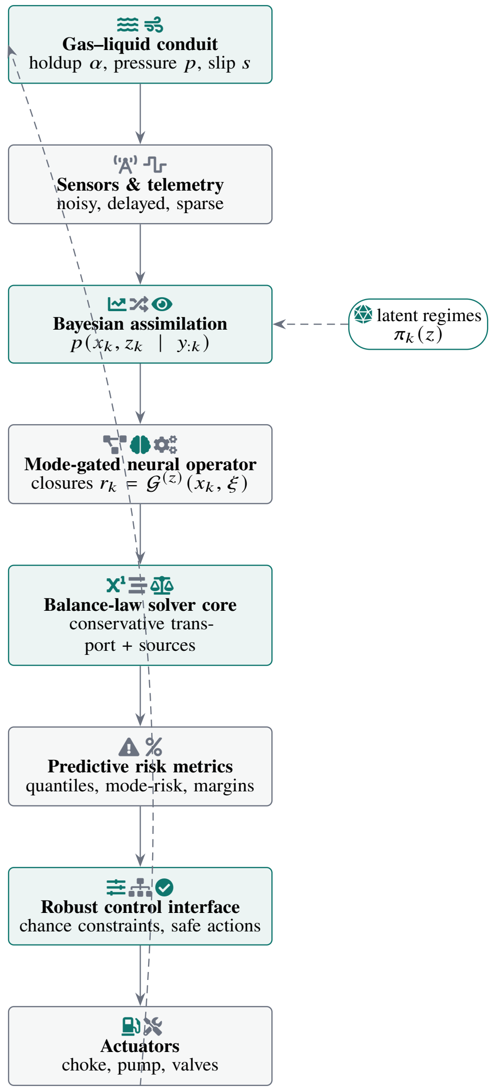

Figure 1 End-to-end real-time digital-twin loop for gas–liquid two-phase flow: sparse measurements are assimilated into a regime-switching probabilistic state estimate, which gates physics-constrained neural-operator closures embedded in a conservative balance-law solver; predictive risk summaries drive a robust control interface for choke/pump actuation with uncertainty-aware safety margins.

creates hysteresis and path dependence that are not naturally captured by single-regime closures.

Traditional modeling approaches span mechanistic two-fluid formulations, drift-flux variants, and empirical correlations calibrated for restricted operating envelopes [2]. They offer interpretability and can extrapolate across modest changes, but they become brittle when confronted with uncertain closure parameters, unmodeled geometry effects, and transient events such as gas influx, choke adjustments, or rapid ramping of pump rates. At the other extreme, purely data-driven models can fit complex mappings but may violate conservation constraints, become unstable when extrapolating beyond the training distribution, and provide limited guidance for control design. A useful digital twin for two-phase flow must therefore combine the inductive bias of conservation laws with data-adaptive components that learn closures and transition behavior from heterogeneous measurements.

The present paper argues that the right abstraction for this combination is a regime-switching stochastic dynamical system in which discrete latent modes represent regime-dependent closure families, while continuous states represent averaged phase variables and momentum. This abstraction permits the system to exhibit sharp changes in response without requiring the underlying continuous state to be discontinuous [3]. It also creates a natural interface to probabilistic inference, because uncertainty can be decomposed into continuous-state uncertainty within a mode and discrete uncertainty over modes. While many operational workflows treat regime identification as a separate classification stage, a twin that is intended to support control should instead treat regime as a latent variable that is inferred jointly with physical state, because the correct mode is itself uncertain and evolves in time.

Data-driven regime mapping remains important, but it is most valuable when integrated into a dynamical estimator rather than used as a static lookup. In this context, prior work has shown that high-accuracy machine learning classifiers can identify gas–

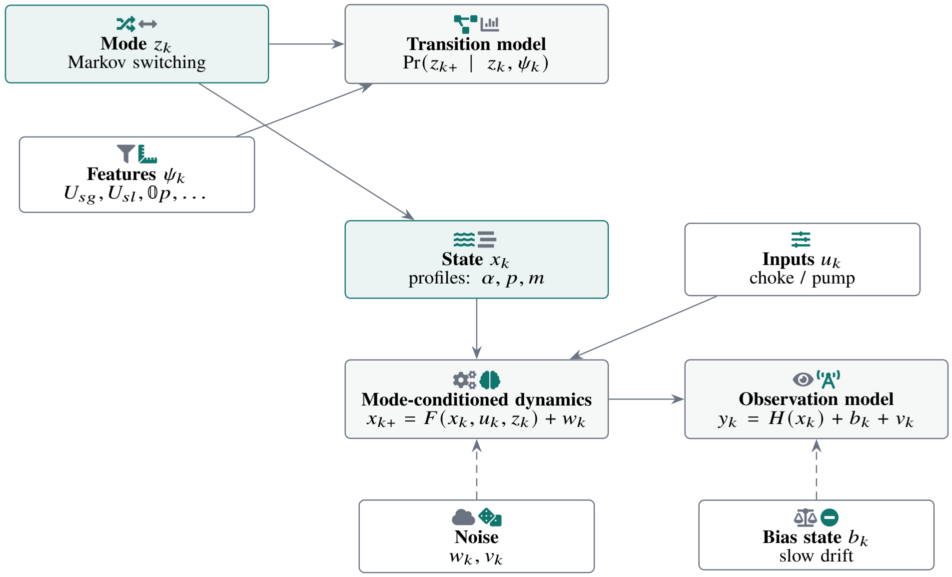

Figure 2 Regime-switching state-space abstraction: a discrete latent mode z_k evolves via condition-dependent transitions driven by features ψ_k, while continuous averaged states x_k propagate through mode-conditioned dynamics under control inputs; measurements are explained by an observation model with explicit bias states to prevent spurious mode switching under systematic sensor error.

Layer	Description	Representative variables
Mechanistic core	Semi-discrete mass and momentum balance laws	$x_k,\ q(x),\ f(x,z),\ s(x,u,z,\theta)$
Neural-operator closures	Mode-gated nonlocal closure functionals	$\mathcal{G}_\theta^{(z)},\ r_k$
Regime process	Latent Markov chain with condition-dependent transitions	$z_k,\ \alpha_{ij},\ \psi_k$
Bayesian assimilation	Joint state–mode filter with sensor-bias tracking	$\mu_{k\|k}^{(z)},\ P_{k\|k}^{(z)},\ \pi_k(z),\ b_k$
Robust control interface	Chance-constrained receding-horizon optimization	$u_{k:k+N-},\ \ell(\cdot),\ g(\cdot),\ \delta$

Table 1 Overview of the main components in the regime-switching neural-operator digital twin.

liquid flow regimes from experimental and historical datasets, including cases where annular-regime discrimination is required in annular channel geometries; Manikonda et al. (2021) provided an early demonstration of such supervised classification pipelines achieving strong predictive accuracy for multiple regimes [4]. That line of work motivates the present effort but does not define it: the focus here is not regime classification as an end goal, but the construction of a physically grounded, uncertainty-aware dynamical twin that can ingest noisy measurements, quantify predictive risk, and expose a robust control interface.

The technical contribution of this paper is a unified architecture that links four components into a coherent system. The first component is a continuous-time or discrete-time two-phase state representation derived from conservation balances, written in a form suitable for online propagation under control inputs. The second is a physics-constrained neural operator that approximates closure relations as nonlocal functionals of the state, enabling geometry and regime dependence without sacrificing conservation structure. The third is a mode transition model that treats regime as a latent Markov process whose transition intensities depend on physically interpretable features such as superficial velocities and pressure gradients [5]. The fourth is a Bayesian assimilation layer that performs joint inference over continuous states, closure parameters, and regime probabilities, producing predictive distributions that can be used for robust control.

The remainder of the paper develops this framework in a way that is intended to be implementable in real systems. The modeling section formalizes a compact yet expressive representation of two-phase dynamics, emphasizing the separation between conserved quantities and closure functionals. The hybrid learning section introduces a neural-operator parameterization that is constrained by residual minimization of conservation laws and by stability conditions for wave propagation. The inference section derives a joint filtering scheme and discusses identifiability and calibration, with attention to the realities of biased sensors and intermittent telemetry [6]. The control section develops a robust decision interface that uses the twin as a probabilistic predictor inside a constrained optimization loop, while maintaining safety constraints under uncertainty. Throughout, the paper prioritizes mechanisms that allow the twin to adapt online without producing physically nonsensical states, such as negative phase fractions or unstable pressure responses.

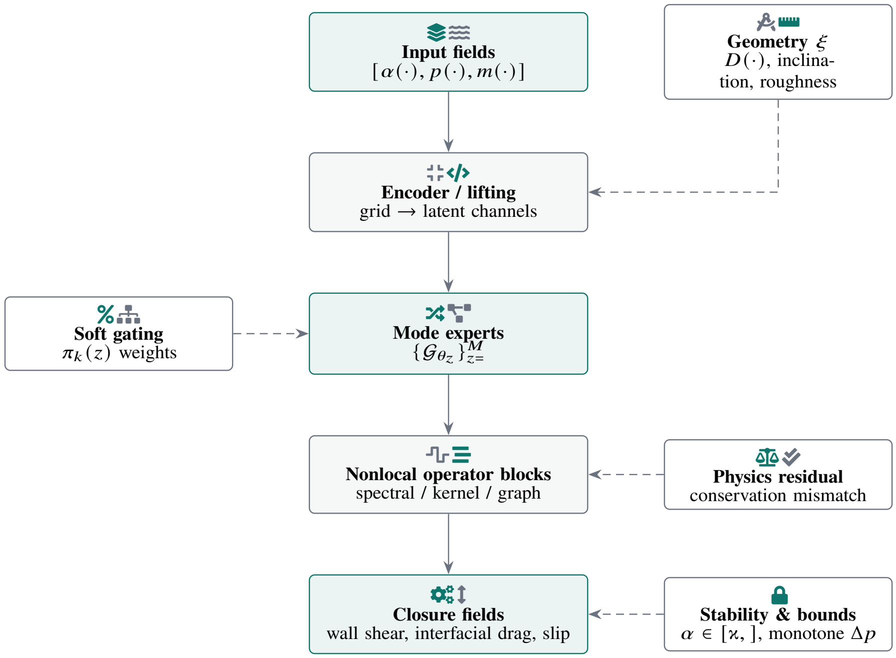

Figure 3 Physics-constrained neural-operator closure surrogate: state fields are lifted to latent channels, processed by mode-specialized operator experts with soft probabilistic gating, and decoded into distributed closure fields; conservation residual penalties and stability/boundedness constraints regularize learning so the embedded solver remains physically plausible under regime changes and geometry variation.

Symbol	Meaning	Domain / type
x_k	Discretized state (holdup, momentum, pressure profiles)	$\mathbb{R}^{n_x}$
u_k	Control input (choke, pump, gas-lift settings)	$\mathbb{R}^{n_u}$
y_k	Measurement vector (pressures, rates, acoustic signals)	$\mathbb{R}^{n_y}$
z_k	Latent flow regime / mode index	$\{, \dots, M\}$
θ	Closure and operator parameters	$\mathbb{R}^{n_\theta}$
ϕ	Sensor model parameters	$\mathbb{R}^{n_\phi}$
ξ	Geometry and configuration descriptors	$\mathbb{R}^{n_\xi}$

Table 2 Key notation for state, control, measurement, and parameter variables in the proposed framework.

2. Modeling Framework for Two-Phase Digital Twins

A digital twin for gas–liquid flow must represent the evolution of averaged phase quantities along a conduit, together with the influence of control actions and boundary conditions. Let the spatial domain be an interval along the flow direction, and let the state encode cross-sectionally averaged variables for each phase. A minimal representation includes the liquid holdup, phase superficial velocities, and pressure, but the representation can be expanded to include mixture temperature, compressibility effects, and entrained fractions if the application requires them [7]. The key modeling choice is to write the evolution as a balance law with closure functionals that capture interfacial momentum transfer and wall friction. This makes the conservation structure explicit, while isolating the uncertain components into mappings that can be learned.

To fix ideas, consider a reduced one-dimensional representation in which the continuous state at time index k is a vector x_k collecting discretized holdup, mixture momentum, and pressure along the conduit. Control inputs u_k represent manipulated variables such as choke opening, pump rate, or gas lift. Measurements y_k are produced by sensors that may include pressure transducers, flow meters, acoustic measurements, and occasional estimates of phase fractions [8]. In practice, the measurement operator can be nonlinear, biased, and subject to delays; the model must therefore accommodate observation uncertainty and potential mismatch between the sensor model and reality.

We propose to represent the twin dynamics with a mode-conditioned evolution operator. A latent discrete variable z_k takes values in a finite set of modes corresponding to regime-

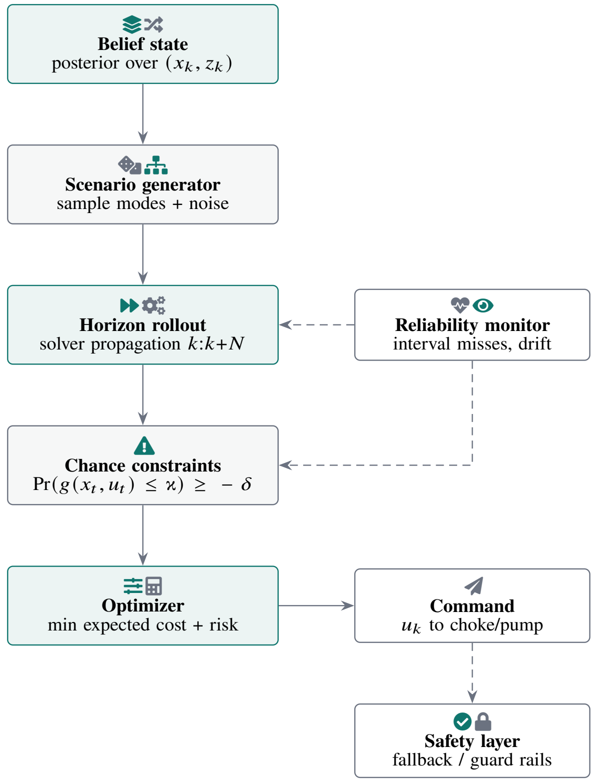

Figure 4 Robust decision interface built on the probabilistic twin: scenario ensembles sampled from the switching posterior are rolled forward through the physics-constrained model, enabling chance-constrained optimization of choke/pump actions; reliability monitoring inflates uncertainty or triggers safety layers when calibration degrades.

dependent closure families. The dynamics are written as

$$\begin{aligned} x_{k+} &= F(x_k, u_k, z_k, \theta) + w_k \\ y_k &= H(x_k, \phi) + v_k \end{aligned} \tag{1}$$

where θ parameterizes closure models, ϕ parameterizes the sensor model, and w_k and v_k represent process and observation noise [9]. The function F is not an arbitrary neural network; it is constructed from a mechanistic discretization of balance laws plus a learnable closure operator. This construction preserves the meaning of the state variables and provides a structured route to stability analysis, while still allowing the twin to adapt to complex regimes and geometries.

A useful decomposition writes the update as a sum of a conservative transport component and a source component. Let $q(x)$ denote a vector of conserved densities, and let $f(x,z)$ denote mode-dependent fluxes. A generic semi-discrete form can be expressed as [10]

$$\begin{aligned} q_{k+} = q_k &- \Delta t\, D\, f(x_k, z_k) \\ &+ \Delta t\, s(x_k, u_k, z_k, \theta) + \eta_k \end{aligned} \tag{2}$$

where D is a discrete divergence operator, $s(\cdot)$ collects source terms, and η_k aggregates discretization and model errors. The dependence on θ is concentrated in the closure contribution to f and s, such as friction factors, interfacial shear, and slip relations. This separation is important because it permits learning to focus on closures rather than on rewriting the conservation structure from scratch. It also allows the twin to enforce invariants such as bounded phase fractions and to maintain consistent pressure evolution under compressibility constraints.

The mode variable z_k is modeled as a controlled Markov chain. Rather than using a fixed transition matrix, which would ignore the influence of operating conditions, we define condition-dependent transitions [11]. Let ψ_k be a feature vector derived from x_k and u_k, for example superficial velocities, dimensionless groups, and local gradients. The transition probability is

$$\Pr(z_{k+} = j \mid z_k = i, \psi_k) = \frac{\exp(\alpha_{ij}^\top \psi_k)}{\sum_m \exp(\alpha_{im}^\top \psi_k)} \tag{3}$$

where α_{ij} are learnable parameters. This parameterization allows the twin to express that some transitions become more likely under higher gas superficial velocity, while others dominate when liquid rate increases. Importantly, the mode is not directly observed; it must be inferred from measurements. Therefore, the transition model must avoid pathological behavior such as rapid oscillation between modes due to noise [12]. We address this by incorporating regularization that penalizes excessive switching and by imposing dwell-time constraints that reflect physical inertia of regime structures.

The closure operator is the primary source of modeling uncertainty. In many systems, closure terms depend not only on local state values but also on upstream conditions, interfacial wave evolution, and geometry features that are not encoded in x_k. This motivates a nonlocal functional representation rather

Term	Definition	Interpretation
$F(x_k, u_k, z_k, \theta)$	Mechanistic step with mode-conditioned closures	Discrete-time evolution of averaged two-phase variables
$H(x_k, \phi)$	Possibly biased, nonlinear observation operator	Mapping from internal state to sensor channels
w_k	Process noise	Unmodeled dynamics and discretization error
v_k	Observation noise	Sensor noise and telemetry uncertainty
$q(x)$	Conserved densities	Cross-sectionally averaged mass / momentum
$f(x, z)$	Mode-dependent fluxes	Convective transport and slip effects
$s(x, u, z, \theta)$	Source terms	Wall friction, interfacial drag, control actuation

Table 3 Discrete-time state–space representation and associated quantities for the digital twin.

Feature in ψ_k	Physical meaning	Typical source
U_{sg}	Superficial gas velocity	Allocated gas-rate and cross-sectional area
U_{sl}	Superficial liquid velocity	Liquid-rate measurements or pump curves
$\mathbb{0}p$	Local pressure gradient	Distributed pressure sensors or inferred profile
Re, Fr	Dimensionless numbers	Derived from fluid properties and velocities
Δu_k	Recent control increments	Differences in choke and pump settings

Table 4 Example features that parameterize the condition-dependent regime transition model.

than a purely local regression. A neural operator provides such a representation: it maps an input field, such as holdup and velocity profiles, to an output field, such as friction and slip parameters, with built-in capacity to represent long-range dependencies [13]. In this framework, the neural operator is conditioned on the mode z_k and potentially on geometry descriptors, enabling different closure behavior in different regimes and conduits. The next section details the construction of this operator and the constraints required to maintain physical plausibility.

3. Physics-Constrained Regime-Switching Neural Operators

A central design goal is to learn flexible closure mappings without letting the twin violate conservation laws or become dynamically unstable. Neural operators provide a natural balance: they can learn mappings between function spaces while preserving the structure of discretized PDE solvers when embedded correctly. We introduce a mode-gated neural operator $\mathcal{G}_\theta^{(z)}$ that maps state fields to closure fields. The operator can be implemented via spectral convolution, kernel integral forms, or graph-based message passing over the spatial grid, but the defining property is that it approximates a nonlocal functional rather than a pointwise map [14].

Let r_k denote the collection of closure fields required by the discretization at time k, such as wall shear coefficients, interfacial drag terms, and slip multipliers. We define

$$r_k = \mathcal{G}_\theta^{(z_k)}(x_k, \xi) + \epsilon_k \tag{4}$$

where ξ encodes fixed descriptors such as diameter profile, inclination, and roughness, and ϵ_k captures residual uncertainty. The state update is then written as a solver step that uses r_k to evaluate fluxes and sources. This makes learning modular: improvements to $\mathcal{G}$ improve the twin while leaving the conservation core intact.

To train the operator, we combine data fitting with physics residual constraints [15]. Suppose a dataset contains sequences of states and observations obtained from simulations, experiments, or operations. Direct supervision on r_k is rarely available, because closure fields are not measured; therefore, training must rely on matching observed outputs and minimizing the residual of the discretized balance laws. We define a loss functional consisting of a measurement term and a physics term. The measurement term penalizes mismatch between predicted measurements and actual measurements under the observation model. The physics term penalizes the violation of balance laws when the predicted closures are applied [16]. A representative form is

$$\begin{aligned}\mathcal{L}(\theta, \phi) = \sum_k \|y_k - H(x_k, \phi)\|_{R^{-}} \\ + \lambda \sum_k \|\mathcal{R}(x_{k+}, x_k, u_k, r_k)\|\end{aligned} \tag{5}$$

where x_k is the predicted state, R is an observation covariance, $\mathcal{R}$ is the discrete residual operator, and λ balances the two terms. The residual operator is constructed directly from the discretization, so its minimization enforces that the learned closures yield approximately conservative evolution.

Mode gating is introduced through a mixture-of-experts structure. Each mode z has an associated operator $\mathcal{G}_{\theta_z}$, but

Aspect	Option A	Option B	Option C
Purpose			
Kernel family	Spectral convolution	Integral operator	Graph message passing
Capture nonlocal closure behavior			
Mode handling	Hard gating	Soft mixture of experts	Shared base $+\Delta$ per mode
Control specialization vs. identifiability			
Geometry encoding	Global scalars	Axial profiles	Learned embeddings
Represent diameter, inclination, roughness			
Regularization	Lipschitz penalties	Monotonicity constraints	Dwell-time-aware loss
Promote stability and physical plausibility			

Table 5 Design choices for the regime-conditioned neural operator and associated regularization strategies.

Loss term	Example expression	Role in training
Measurement fit	$\sum_k \|y_k - H(x_k, \phi)\|_{R^-}$	Match predicted and observed sensor channels
Physics residual	$\lambda \sum_k \|\mathcal{R}(x_{k+}, x_k, u_k, r_k)\|$	Enforce approximate conservation laws
Mode regularization	$\gamma \sum_k \mathrm{KL}(\pi_k \,\|\, \pi_{\mathrm{ref}})$	Discourage implausible switching patterns
Operator complexity	$\eta \|\Delta \mathcal{G}_{\theta_z}\|$	Encourage parsimonious mode differences
Parameter prior	$\beta\, \mathrm{KL}(q(\theta) \,\|\, p(\theta))$	Embed physical priors and avoid overfitting

Table 6 Representative loss components used to train the physics-constrained, regime-switching neural operator.

hard assignment is undesirable during training because mode labels may be absent. Instead, we use soft gating weights $\pi_k(z)$ representing the probability that the system is in mode z at time k. The effective closure is then [17]

$$r_k = \sum_z \pi_k(z)\, \mathcal{G}_{\theta_z}(x_k, \xi) \tag{6}$$

where $\pi_k(z)$ can be produced by an auxiliary inference network or by the Bayesian filter described later. Soft gating allows gradients to flow to all mode operators while still encouraging specialization. It also reflects operational reality: regimes are not perfectly separable, and mixed structures can occur near transition boundaries.

Stability and physical plausibility require additional constraints beyond residual minimization. One requirement is boundedness of holdup and phase fractions, which can be violated by naive neural surrogates [18]. We enforce bounds by parameterizing holdup in a transformed space and mapping back through a squashing function, while ensuring that the conservative update respects these bounds. Another requirement concerns monotonicity of pressure drop with respect to frictional closures in steady segments, which can be encoded as inequality constraints on the operator outputs. Because strict inequality constraints are difficult to enforce exactly, we incorporate penalty terms that discourage violations in regions of the state space where monotonicity should hold.

A further challenge is the entanglement between regime switching and closure variability. If the operator is too expressive, it can mimic the effect of switching by changing its output smoothly, making the mode variable redundant [19]. Conversely, if the mode variable is too flexible, it can absorb closure errors by switching frequently. We address this identifiability issue through structural constraints. Mode operators are encouraged to differ primarily in a low-dimensional subspace that corresponds to interpretable closure variations, while within-mode variability is restricted by smoothness and Lipschitz penalties. A simple formalization introduces a shared base operator plus mode-specific residuals:

$$\mathcal{G}_\theta^{(z)} = \mathcal{G}_{\theta_\varkappa} + \Delta \mathcal{G}_{\theta_z} \tag{7}$$

and penalizes the norm of $\Delta \mathcal{G}_{\theta_z}$ to avoid arbitrary divergence unless supported by data. This helps the mode variable retain semantic meaning as a switch between qualitatively different closure families rather than a free index.

The approach is compatible with regime identification results from the literature, but it reframes regime as an internal latent that interacts with dynamics and uncertainty [20]. In a related horizontal-flow context, Manikonda et al. (2022) [21] showed that carefully tuned machine learning classifiers can separate multiple horizontal gas–liquid regimes with high predictive accuracy and can resolve annular-channel patterns as part of the regime set. In the present framework, such discriminative capability is valuable as an informative prior or as a feature generator

Block	Variables	Approximation	Notes
Prediction	$x^{(z)}_{k\|k-}, P^{(z)}_{k\|k-}$	Linearization or sigma points	Mode-conditioned state propagation
Measurement update	$x^{(z)}_{k\|k}, P^{(z)}_{k\|k}$	Extended / unscented update	Incorporates sensor noise and bias
Mode probability	$\pi_k(z)$	Discrete Bayes' rule	Uses mode-specific likelihoods and transitions
Bias tracking	b_k	Slow random walk	Captures persistent sensor offsets
Parameter adaptation	$q(\theta)$	Online variational updates	Low-dimensional fast calibration, slower global updates

Table 7 Structure of the Bayesian assimilation scheme combining continuous-state filtering, mode inference, and parameter adaptation.

Element	Symbol / example	Description
Horizon length	N	Number of future steps in the receding-horizon optimization
Stage cost	$\ell(x_t, u_t)$	Penalizes pressure tracking error and actuator movement
Constraints	$g(x_t, u_t) \leq \varkappa$	Safety limits on pressures, flow rates, and holdup
Risk tolerance	δ	Maximum allowed probability of constraint violation
Control limits	$u_{\min} \leq u_t \leq u_{\max}$	Bounds on choke openings and pump rates

Table 8 Key ingredients of the chance-constrained robust control formulation used with the digital twin.

for the mode transition model, but the twin ultimately treats regimes probabilistically and couples them to state evolution to support robust forecasting and control.

4. Bayesian Assimilation, Identifiability, and Calibration

A digital twin becomes operationally useful when it can assimilate new measurements online, correct model drift, and quantify uncertainty in forecasts. This paper adopts a Bayesian perspective in which the state, mode, and model parameters are treated as random variables conditioned on the measurement history [22]. The key object is the filtering distribution

$$p(x_k, z_k, \theta \mid y_{:k}, u_{:k-}) \tag{8}$$

from which one can compute predictive distributions for future states and measurements. Exact inference is intractable because the dynamics are nonlinear and include discrete modes, so we develop an approximate filter that combines continuous-state Gaussian approximations with discrete mode probability updates, along with parameter adaptation on a slower time scale.

We begin by separating the inference into two coupled recursions: one for the continuous state conditioned on a mode, and one for the mode probabilities. Given mode z_k, we approximate the state evolution locally with a linearization or with sigma-point propagation, depending on computational constraints [23]. Let the conditional predictive density be approximated as Gaussian with mean $\mu^{(z)}_{k|k-}$ and covariance $P^{(z)}_{k|k-}$. The measurement update then yields $\mu^{(z)}_{k|k}$ and $P^{(z)}_{k|k}$ through a standard nonlinear filtering step. The mode probabilities are updated using Bayes' rule with the measurement likelihood under each mode:

$$\begin{aligned}\pi_k(z) \propto \Pr(z_k = z \mid z_{k-}) \\ \times p(y_k \mid \mu^{(z)}_{k|k-}, P^{(z)}_{k|k-})\end{aligned} \tag{9}$$

followed by normalization. This update couples the mode to the quality of the measurement prediction: modes that better explain the observed sensor behavior become more probable. The transition term uses the condition-dependent model introduced earlier, which is itself a function of estimated features.

In practice, measurement models can include biases, scale factors, and time offsets [24]. A naive filter that assumes unbiased sensors will attribute systematic errors to state changes or mode switching, which can lead to persistent misclassification and drift. We therefore include a bias state b_k for selected sensors and treat it as a slowly varying random walk. The observation model becomes $y_k = H(x_k, \phi) + b_k + v_k$, and the filter jointly estimates b_k with x_k. This modification improves calibration because it prevents the twin from compensating for sensor bias by adjusting closures or switching modes inappropriately.

Parameter adaptation is handled with an online variational approximation [25]. Let θ include both operator parameters and transition parameters. Full online learning of a high-capacity operator can be unstable and computationally heavy, so we separate θ into fast and slow components. The fast component includes low-dimensional calibration parameters such as friction multipliers, while the slow component includes the high-dimensional operator weights. Online updates are applied primarily to the fast component, while the slow component is updated in batched intervals or via low-rank adapters. Formally, we define a variational family $q(\theta)$ and minimize an evidence lower bound that incorporates the filtering likelihood [26]. The

Scenario	Perturbation	Primary metric	Observed behavior
Baseline tracking	Nominal sensors and geometry	RMSE, NLL, constraint violations	Hybrid twin provides calibrated
Sensor dropout	Removal of subset of pressure channels	Forecast error, interval coverage	Mechanistic core maintains bou
Geometry shift	Change in diameter / inclination profile ξ	Performance across envelopes	Geometry-aware operator adapts
Regime ambiguity	Operation near transition boundaries	Mode entropy, safety violations	Mixed mode probabilities and c
Telemetry bias	Slowly drifting sensor offset	Calibration diagnostics	Bias state b_k absorbs drift, prev

Table 9 Illustrative stress-test scenarios used to evaluate forecasting reliability and control performance under realistic deployment conditions.

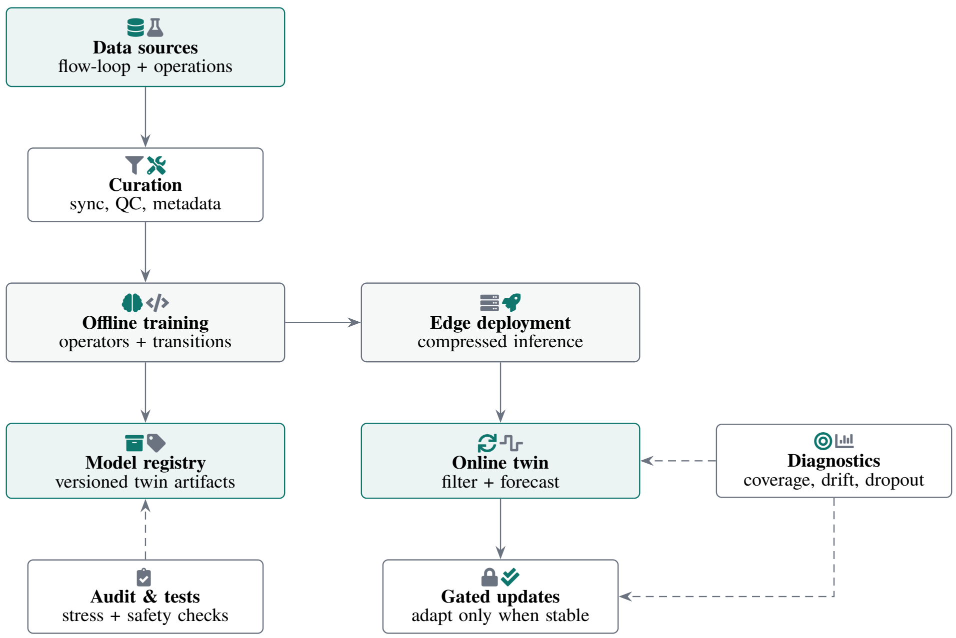

Figure 5 Practical deployment workflow: heterogeneous experimental and operational datasets are curated for offline training of regime-switching operator components, producing versioned artifacts for edge deployment; online inference runs with diagnostics and gated adaptation to maintain reliability under sensor dropout and distribution shift.

update takes the form of a stochastic gradient step on

$$\mathcal{J}(\theta) = -\sum_k \log p(y_k \mid y_{:k-}, u_{:k-}, \theta) + \beta\,\mathrm{KL}(q(\theta) \,\|\, p(\theta)) \tag{10}$$

where $p(\theta)$ is a prior encoding physical plausibility and β controls regularization strength. The prior plays a practical role: it discourages parameter values that would produce nonphysical holdup or unstable pressure propagation, and it reduces overfitting to short-term noise.

Identifiability is a crucial question because the twin contains multiple mechanisms that can explain the same observation. For example, an unexpected pressure drop could be explained by increased friction closure, by a change in holdup affecting hydrostatic head, or by a mode change to a regime with different slip [27]. If the inference machinery cannot distinguish these explanations, the twin will remain uncertain and may oscillate between hypotheses. We provide conditions under which the mode and closure parameters become identifiable from available measurements. The core idea is that identifiability requires excitation across operating conditions and observability of the effects of each mechanism on the measured outputs. If only pressure is measured at a single location, then multiple internal configurations can produce the same reading. If, however, pressures at multiple locations and flow rates are measured, then the spatial structure of pressure gradients can distinguish friction changes from holdup changes, and transient responses to control steps can distinguish mode changes from smooth parameter drift [28].

A useful diagnostic is the Fisher information associated with the measurement likelihood under the filtered state distribution. Modes that are hard to distinguish will yield similar likelihood gradients with respect to the data, leading to low information for mode discrimination. The twin can detect such situations and maintain a multimodal mode distribution rather than forcing a premature hard decision. This behavior is operationally desirable because it represents uncertainty honestly and can be propagated into control decisions. Calibration of the predictive distribution is assessed by checking whether empirical coverage of prediction intervals matches nominal coverage over held-out sequences

[29]. When coverage is poor, the twin can adapt noise models or adjust regularization to avoid overconfident predictions.

Because regime switching is treated probabilistically, the twin can produce forecasts that marginalize over possible future modes. The one-step predictive distribution is

$$\begin{aligned} p(x_{k+} \mid y_{:k}) = \sum_{z} \int & p(x_{k+} \mid x_k, z, \theta) \\ & \times p(x_k, z, \theta \mid y_{:k})\, dx_k\, d\theta \end{aligned} \tag{11}$$

which is approximated in implementation by a mixture of Gaussians or by particle-based sampling over modes. This forecast is what feeds the control interface: the controller does not receive a single predicted pressure profile, but rather a distribution that encodes both continuous uncertainty and the possibility of regime transitions.

5. Robust Control Interfaces and Safety-Constrained Decision Support

A principal motivation for building a probabilistic digital twin is to inform control actions under uncertainty [30]. In drilling and production contexts, actuators such as chokes, pumps, and valves can induce rapid changes that interact with two-phase dynamics in nonlinear ways. A controller that ignores regime uncertainty may apply an action that is safe under one regime but unsafe under another. Conversely, overly conservative control can degrade performance. The proposed twin provides a structured compromise by enabling optimization over expected performance while enforcing probabilistic safety constraints.

We frame control as a receding-horizon optimization [31]. At time k, given the filtering distribution over the current state and mode, we choose a sequence of controls $u_{k:k+N-}$ to minimize an objective while respecting constraints. The objective can encode tracking of desired pressure, minimization of oscillations, and penalties for actuator movement. Constraints can include upper bounds on pressure, lower bounds on bottomhole pressure relative to formation pressure margins, and bounds on flow rates. Because the twin provides a predictive distribution, constraints are enforced in a chance-constrained sense. A representative formulation is

$$\begin{aligned} \min_{u_{k:k+N-}} \ & \mathbb{E}\Big[\sum_{t=k}^{k+N-} \ell(x_t, u_t) \Big] \\ \text{s.t.} \ \ & \Pr(g(x_t, u_t) \leq \varkappa) \geq \ -\delta \end{aligned} \tag{12}$$

where ℓ is a stage cost, g encodes constraints, and δ is a risk tolerance [32]. The expectation and probability are taken with respect to the predictive distribution produced by the twin.

Implementing chance constraints requires approximations. One approach is to propagate a set of representative scenarios sampled from the mode-conditioned predictive distribution. Each scenario corresponds to a sampled mode sequence and sampled process noise, and the mechanistic core of the twin propagates the state forward under candidate controls. Constraints are then enforced across the scenario set, either by requiring all scenarios to satisfy constraints or by allowing a small fraction to violate them consistent with δ [33]. A complementary approach uses analytic approximations when the predictive distribution is approximately Gaussian within each mode, by linearizing constraints and using quantiles of the resulting distribution. The scenario approach is more robust to multi-modality induced by regime switching, which is common in the present setting.

Safety constraints often involve limits that must hold continuously, not just at discrete time points, and they may depend on unmeasured internal variables such as local holdup. The twin addresses this by predicting internal profiles and their uncertainty, enabling constraints on derived quantities. For example, one can constrain the probability that holdup exceeds a threshold associated with severe slugging risk, even if holdup is not directly measured [34]. Such constraints are necessarily model-dependent, but the physics-constrained operator and the calibration procedures described earlier reduce the risk of gross misprediction.

An important interface question is how to communicate uncertainty to operators or automation layers. A twin that returns only a mean forecast can conceal risk, while a twin that returns full distributions may be too complex for real-time decision-making unless summarized effectively. We propose to expose a small set of risk metrics derived from the predictive distribution, such as the predicted upper quantile of pressure at critical locations and the probability of entering a high-risk mode within the horizon. These metrics can be computed from the scenario ensemble and updated at each control step [35]. The control system can then adjust aggressiveness based on risk. When risk is low, the controller can prioritize performance, and when risk rises, it can shift toward conservative actions that reduce the probability of constraint violation.

Robustness to model mismatch is addressed by incorporating adaptive safety margins. If the twin detects calibration degradation, for instance by observing that realized measurements fall outside predicted intervals too frequently, it can increase process noise or inflate predictive covariance. This inflation increases conservativeness of chance constraints automatically, providing a principled response to loss of model reliability [36]. The controller thus remains safe even when the twin encounters unseen operating conditions, at the cost of reduced performance until the twin adapts through online learning.

A further benefit of the regime-switching representation is that it supports mode-aware control logic without hard-coded regime thresholds. In many practical systems, operators apply different heuristics in different regimes, such as damping actions when slugging is likely. In our framework, this behavior can be obtained by allowing the stage cost to depend on the mode probability distribution. For example, actuator movement can be penalized more strongly when the probability of an oscillatory regime is high [37]. Because mode is uncertain, the cost becomes an expectation over modes, leading to smooth transitions in control behavior rather than abrupt switches based on potentially noisy regime labels.

Finally, the control interface can be coupled with a decision-support layer for contingency management. In well control, for instance, actions may include reducing pump rate, adjusting choke, or initiating specific procedures when influx is suspected.

The twin can compute the posterior probability of abnormal events by comparing likelihood under nominal and abnormal models, and it can forecast the consequences of candidate actions under uncertainty. This supports a rational allocation of attention and intervention, especially when sensor noise and regime ambiguity could otherwise produce false alarms [38]. The key point is that decision support is anchored in the same probabilistic dynamical model used for prediction and control, avoiding inconsistencies that arise when classification, forecasting, and control are treated as separate black boxes.

6. Computational Study, Stress Tests, and Practical Deployment Considerations

To assess the value of the proposed digital-twin framework, we consider computational experiments designed to mimic realistic conditions: heterogeneous datasets, partial observability, sensor bias, and distribution shift across geometries and operating envelopes. The goal is not to claim universal superiority, but to evaluate whether the hybrid structure provides measurable gains in predictive reliability and control-relevant performance relative to plausible alternatives. We therefore compare the full regime-switching neural-operator twin to baselines that remove specific components, such as a mechanistic-only model with fixed closures, a neural surrogate without physics residual constraints, and a single-mode hybrid model without regime switching.

The evaluation focuses on two families of tasks. The first family is forecasting and state estimation: given historical measurements and control inputs, how accurately does the twin predict future pressure and holdup distributions, and how well-calibrated are its uncertainty intervals [39]. The second family is control: when embedded in a receding-horizon controller, how often are safety constraints violated, and what is the achieved performance in terms of tracking and actuator usage. For forecasting tasks, the primary metrics include root-mean-square prediction error on measured channels, empirical coverage of prediction intervals, and negative log-likelihood of measurements under the predicted distribution. For control tasks, metrics include constraint violation frequency and magnitude, as well as a cost that reflects deviation from desired setpoints and actuator smoothness.

A key stress test is sensor dropout. In many deployments, certain sensors may fail intermittently or become unavailable due to telemetry bandwidth limitations [40]. A purely data-driven surrogate trained on dense sensor inputs can degrade sharply when inputs are missing. The proposed twin is more robust because it propagates the state using the mechanistic core and updates using whatever measurements remain, while uncertainty grows appropriately. In experiments where a subset of pressure sensors is dropped for extended intervals, the regime-switching hybrid twin maintains bounded forecast errors and produces wider prediction intervals that remain calibrated. In contrast, the neural surrogate without conservation constraints can drift into nonphysical states, and its uncertainty estimates, if any, tend to be miscalibrated because the model was not trained to represent missing-data uncertainty explicitly.

Another stress test is distribution shift across geometry [41]. Operational systems may differ from training systems in diameter, inclination, roughness, or sensor placement. The inclusion of geometry descriptors ξ in the neural operator allows the twin to condition closures on these differences, but only if the operator has been trained across a range of descriptors or if online adaptation can compensate. We therefore evaluate performance under moderate shifts in ξ and under shifts in operating envelope. The regime-switching structure helps because certain regimes manifest similarly across geometries at the level of qualitative dynamics, even if quantitative closures differ; mode probabilities can transfer while closure parameters adapt. The physics residual constraints further stabilize adaptation by limiting the space of plausible closure updates [42].

A third stress test targets regime ambiguity near transition boundaries. Near such boundaries, small perturbations can alter the observed dynamics, and static regime labels can be inconsistent. The proposed twin naturally represents this ambiguity through a mixed mode distribution. Forecasts become mixtures that reflect competing hypotheses, and the controller can act conservatively when risk is high. In computational experiments, this behavior reduces constraint violations compared to a controller that commits to a single regime estimate [43]. It also reduces unnecessary aggressive actions in cases where the system could plausibly be in a more benign regime. The benefit is most pronounced when measurements are noisy and when the action-induced dynamics can push the system across a transition boundary.

Practical deployment requires attention to computational cost. Neural operators can be heavy if implemented at high resolution, and Bayesian filtering across multiple modes can multiply the cost further. The proposed framework mitigates this by using a coarse grid for online propagation and reserving fine-grid computation for offline training and periodic recalibration [44]. The operator itself can be compressed through low-rank approximations, weight sharing across modes, and quantization, while maintaining the residual constraints as a guardrail. Mode-conditioned filtering can be limited to a small number of dominant modes at each time step by truncating low-probability modes, which reduces cost while preserving most of the uncertainty mass.

Another deployment issue is data governance and continual learning. Online adaptation is beneficial, but uncontrolled updates can cause regression, especially if the twin is updated on biased or anomalous data. The paper therefore advocates a gated learning policy in which online updates are permitted only when calibration diagnostics indicate stable behavior and when the inferred regime distribution is sufficiently confident [45]. When uncertainty is high, the twin prioritizes safety by inflating uncertainty rather than updating parameters aggressively. Periodic offline retraining can then incorporate new data with proper validation.

Finally, deployment in safety-critical settings demands interpretability. While neural operators are less transparent than simple correlations, the hybrid structure retains interpretability through the mechanistic state and through physically meaningful closure outputs. Operators can inspect predicted holdup profiles, inferred regime probabilities, and closure fields such as effective friction [46]. When anomalies occur, the twin can attribute them to mode changes, parameter drift, or sensor bias, which supports troubleshooting. This interpretability is not absolute, but it is materially improved relative to an end-to-end black-box predictor because the model exposes internal variables that correspond to physical concepts.

7. Conclusion

This paper introduced a regime-switching, physics-constrained neural-operator digital twin for gas–liquid two-phase flow aimed at real-time forecasting, uncertainty quantification, and robust control integration. The central idea is to treat flow regime as a latent dynamical mode that gates closure functionals while preserving conservation structure in the continuous state evolution. By embedding a neural operator inside a mechanistic balance-law core, the twin can learn nonlocal closure behavior and geometry dependence without sacrificing physical plausibility [47]. A Bayesian assimilation layer performs joint inference over continuous states, sensor biases, and mode probabilities, producing calibrated predictive distributions that propagate both continuous and discrete uncertainty. These distributions support chance-constrained control and decision support, enabling safety-aware actions under ambiguity and sensor imperfections.

Beyond the architectural proposal, the paper emphasized identifiability considerations and stability constraints needed to prevent degenerate explanations in which mode switching mimics closure drift or vice versa. The computational study discussed stress tests that reflect deployment realities, including sensor dropout, distribution shift, and regime ambiguity near transition boundaries, and it highlighted mechanisms for maintaining robustness through uncertainty inflation and gated learning. The resulting framework is not a replacement for mechanistic understanding or for discriminative regime mapping, but rather a unifying layer that integrates physical structure, data-driven adaptability, and probabilistic reasoning into an operationally meaningful twin. Future work within this framework can expand the state representation to incorporate thermal effects and compositional variation, refine transition models using richer features, and develop certification-oriented verification tests for safety-critical automation deployments [48].

Acknowledgments

We would like to thank the reviewers of this research for their helpful comments and suggestions.

References

[1] C. Espinosa, M. Abril, H. Guasch, N. Pou, L. Proia, M. Ricart, M. Ordeix, and L. Llenas, “Water flow and light availability influence on intracellular geosmin production in river biofilms,” *Frontiers in microbiology*, vol. 10, pp. 3002–, 1 2020.

[2] S. Singh, F. Jiang, and T. Tsuji, “Impact of the kinetic boundary condition on porous media flow in the lattice boltzmann formulation,” *Physical review. E*, vol. 96, pp. 013303–, 7 2017.

[3] I. Pană, I. V. Gheţiu, I. G. Stan, F. Dinu, G. Brănoiu, and S. Suditu, “The use of hydraulic fracturing in stimulation of the oil and gas wells in romania,” *Sustainability*, vol. 14, pp. 5614–5614, 5 2022.

[4] K. Manikonda, A. R. Hasan, C. E. Obi, R. Islam, A. K. Sleiti, M. W. Abdelrazeq, and M. A. Rahman, “Application of machine learning classification algorithms for two-phase gas-liquid flow regime identification,” in *Abu Dhabi International Petroleum Exhibition and Conference*, p. D041S121R004, SPE, 2021.

[5] F. Zhu, Z. Lu, and S. Wang, “Flame spread and extinction over a thick solid fuel in low-velocity opposed and concurrent flows,” *Microgravity Science and Technology*, vol. 28, pp. 87–94, 11 2015.

[6] S. Jafari, A. Bouchareb, and T. Nikolaidis, “Thermal performance evaluation in gas turbine aero engines accessory gearbox,” *International Journal of Turbomachinery, Propulsion and Power*, vol. 5, pp. 21–, 8 2020.

[7] W. Lu and A. Davarpanah, “An experimental investigation to consider thermal methods efficiency on oil recovery enhancement,” *Heat Transfer*, vol. 49, pp. 3066–3074, 4 2020.

[8] S. Cui, J. Kong, H. Yu, C. Chen, and J. Wang, “Revising transient-pressure solution for vertical well intersected by a partially penetrating fracture with non-darcy flow effect,” *Geofluids*, vol. 2020, pp. 1–17, 11 2020.

[9] D. Christie, P. Arras, and Z.-Y. Li, “Axisymmetric simulations of hot jupiter–stellar wind hydrodynamic interaction,” *The Astrophysical Journal*, vol. 820, pp. 3–, 3 2016.

[10] A. Riveros, M. Cuellar, P. F. Sánchez, C. Muñoz-Camargo, J. C. Cruz, N. Sandoval, O. D. L. Mejia, and J. C. Briceño, “Design and characterization of a fluidic device for the evaluation of sis-based vascular grafts,” *Processes*, vol. 8, pp. 1198–, 9 2020.

[11] V. Hejtmánek and P. Čapek, “3d microstructure modeling of porous metal filters,” *Metals*, vol. 2, pp. 344–352, 9 2012.

[12] A. S. Palau, S. Eder, T. Andersen, A. K. Ravn, G. Bracco, and B. Holst, “Center-line intensity of a supersonic helium beam,” *Physical Review A*, vol. 98, pp. 063611–, 12 2018.

[13] C. Ferroni, M. Bracconi, M. Ambrosetti, M. Maestri, G. Groppi, and E. Tronconi, “A fundamental investigation of gas/solid heat and mass transfer in structured catalysts based on periodic open cellular structures (pocs).,” *Industrial & engineering chemistry research*, vol. 60, pp. 10522–10538, 6 2021.

[14] L. Zhang, B. Shan, Y. Zhao, J. Du, J. Chen, and X. Tao, “Gas transport model in organic shale nanopores considering langmuir slip conditions and diffusion: Pore confinement, real gas, and geomechanical effects,” *Energies*, vol. 11, pp. 223–, 1 2018.

[15] K. Mahalatkar, J. M. Kuhlman, E. Huckaby, and T. O'Brien, "Simulations of a circulating fluidized bed chemical looping combustion system utilizing gaseous fuel," *Oil & Gas Science and Technology – Revue d'IFP Energies nouvelles*, vol. 66, pp. 301–311, 5 2011.

[16] Y. D. Chashechkin and I. V. Zagumennyi, "2d hydrodynamics of a plate: From creeping flow to transient vortex regimes," *Fluids*, vol. 6, pp. 310–, 8 2021.

[17] A. Diachkovskii, A. Zykova, A. Ishchenko, V. Kasimov, K. S. Rogaev, and A. D. Sidorov, "Mathematical model and software for investigation of internal ballistic processes in high-speed projectile installations," *Journal of Physics: Conference Series*, vol. 919, pp. 012008–, 12 2017.

[18] Z. Guo, R. Wang, and K. Xu, "Discrete unified gas kinetic scheme for all knudsen number flows. ii. thermal compressible case.," *Physical review. E, Statistical, nonlinear, and soft matter physics*, vol. 91, pp. 033313–, 3 2015.

[19] G. Tian, Y. Wu, Z. Sun, D. Jin, H. Song, and M. Jia, "Shock wave boundary layer interaction controlled by surface arc plasma actuators," *Physics of Fluids*, vol. 30, pp. 055107–, 5 2018.

[20] X. Chang, J. Zhou, Y. Guo, H. Shiming, L. Wang, Y. Chen, T. Ming, and R. Jian, "Heat transfer behaviors in horizontal wells considering the effects of drill pipe rotation, and hydraulic and mechanical frictions during drilling procedures," *Energies*, vol. 11, pp. 2414–, 9 2018.

[21] K. Manikonda, R. Islam, C. E. Obi, A. R. Hasan, A. K. Sleiti, M. W. Abdelrazeq, I. G. Hassan, and M. A. Rahman, "Horizontal two-phase flow regime identification with machine learning classification models," in *International Petroleum Technology Conference*, p. D011S021R002, IPTC, 2022.

[22] V. Mosorov, M. Zych, R. Hanus, D. Sankowski, and A. Saoud, "Improvement of flow velocity measurement algorithms based on correlation function and twin plane electrical capacitance tomography.," *Sensors (Basel, Switzerland)*, vol. 20, pp. 306–, 1 2020.

[23] G. Wang, R. Zhang, and L. Cui, "Transient pressure behavior of a horizontal well in a naturally fractured gas reservoir with dual-permeability flow and stress sensitivity effect," *Geofluids*, vol. 2022, pp. 1–11, 4 2022.

[24] "Drying and heating modelling of granular flow: Application to the mix-asphalt processes," *Journal of Applied Fluid Mechanics*, vol. 4, 7 2011.

[25] T. Cao, Y. Duan, R. Wang, L. Zhang, and Q. Fang, "Numerical simulation and production decline analysis of multiply fractured horizontal wells in shale gas reservoirs," *Journal of Engineering Research*, vol. 3, pp. 1–21, 12 2015.

[26] A. Manela and L. Gibelli, "Free-molecular and near-free-molecular gas flows over backward facing steps," *Journal of Fluid Mechanics*, vol. 889, 2 2020.

[27] G. Babac and J. M. Reese, "Knudsen heat capacity," *Physics of Fluids*, vol. 26, pp. 052002–, 5 2014.

[28] A. Blaszczuk, "Effect of flue gas recirculation on heat transfer in a supercritical circulating fluidized bed combustor," *Archives of Thermodynamics*, vol. 36, pp. 61–83, 9 2015.

[29] P. Aussillous, Y. Zhou, P. Ruyer, and P.-Y. Lagrée, "Discharge flow of granular media from silos with a lateral orifice and injection of air," *EPJ Web of Conferences*, vol. 140, pp. 03052–, 6 2017.

[30] Q. Yang and Q. Yang, "Numerical investigation of the turbulence characteristics and energy dissipation mechanism of baffle drop shafts.," *Water science and technology : a journal of the International Association on Water Pollution Research*, vol. 83, pp. 2259–2270, 4 2021.

[31] C. Spurin, T. Bultreys, B. Bijeljic, M. J. Blunt, and S. Krevor, "Mechanisms controlling fluid breakup and reconnection during two-phase flow in porous media.," *Physical review. E*, vol. 100, pp. 043115–, 10 2019.

[32] P. Rostami, M. Sharifi, and M. Dejam, "Shape factor for regular and irregular matrix blocks in fractured porous media," *Petroleum Science*, vol. 17, pp. 136–152, 11 2019.

[33] E. M. Cachaza, M. E. Diaz, F. J. Montes, and M. A. Galán, "Simultaneous computational fluid dynamics (cfd) simulation of the hydrodynamics and mass transfer in a partially aerated bubble column," *Industrial & Engineering Chemistry Research*, vol. 48, pp. 8685–8696, 8 2009.

[34] A. Glière, J. Rouxel, M. Brun, B. Parvitte, V. Zeninari, and S. Nicoletti, "Challenges in the design and fabrication of a lab-on-a-chip photoacoustic gas sensor.," *Sensors (Basel, Switzerland)*, vol. 14, pp. 957–974, 1 2014.

[35] M. Soriano, H. G. Siegel, K. M. Gutchess, C. J. Clark, Y. Li, B. Xiong, D. L. Plata, N. C. Deziel, and J. E. Saiers, "Evaluating domestic well vulnerability to contamination from unconventional oil and gas development sites," *Water Resources Research*, vol. 56, 10 2020.

[36] P. M. Winroth and P. H. Alfredsson, "On shock structures in dynamic exhaust valve flows," *Physics of Fluids*, vol. 31, pp. 026107–, 2 2019.

[37] H. E. Dillon, A. F. Emery, A. M. Mescher, O. Sprenger, and S. Edwards, "Chaotic natural convection in an annular cavity with non-isothermal walls," *Frontiers in Heat and Mass Transfer*, vol. 2, 5 2011.

[38] F. Yi, G. Li, Y. Meng, and B. Guo, "A novel approach to investigating transport of lost circulation materials in rough fracture," *Energies*, vol. 11, pp. 2572–, 9 2018.

[39] Z. S. Spakovszky, "Analysis of aerodynamically induced whirling forces in axial flow compressors," *Journal of Turbomachinery*, vol. 122, pp. 761–768, 2 2000.

[40] R. Wyczółkowski and D. Musiał, "Analysis of the occurrence of natural convection in a bed of bars in vertical temperature gradient conditions," *Archives of Thermodynamics*, vol. 34, pp. 71–83, 3 2013.

[41] S. Z. Ilyas, S. Nasir, and S. Raza, "Air pollution problems and diseases caused by hazardous gases in quetta, pakistan," *Journal of Applied Sciences and Environmental Management*, vol. 12, 6 2010.

[42] A. Rona, "Self-excited supersonic cavity flow instabilities as aerodynamic noise sources," *International Journal of Aeroacoustics*, vol. 5, pp. 335–360, 12 2006.

[43] T. J. Jones, J. K. Russell, and D. Sasse, "Modification of mantle cargo by turbulent ascent of kimberlite," *Frontiers in Earth Science*, vol. 7, pp. 134–, 6 2019.

[44] T. L. Gould, M. R. Tek, and D. L. Katz, "Two-phase flow through vertical, inclined, or curved pipe," *Journal of Petroleum Technology*, vol. 26, pp. 915–926, 8 1974.

[45] J. Sprengel, P. Milano, R. Sfand, and D. Kolak, "Modelling of high point vents in water gathering systems – a new approach using simcenter flomaster," *The APPEA Journal*, vol. 62, pp. 106–115, 5 2022.

[46] W. Tanthapanichakoon, S. Koda, and B. Khemthong, "Dynamic simulation of adiabatic catalytic fixed-bed tubular reactors: A simple approximate modeling approach," *ASEAN Journal of Chemical Engineering*, vol. 14, pp. 25–37, 10 2014.

[47] M. Ricci, R. Pacciani, and M. Marconcini, "The exploitation of cfd legacy for the meridional analysis and design of modern gas and steam turbines," *E3S Web of Conferences*, vol. 197, pp. 11013–, 10 2020.

[48] S. C. Cox, C. D. Menzies, R. Sutherland, P. Denys, C. J. Chamberlain, and D. A. H. Teagle, "Changes in hot spring temperature and hydrogeology of the alpine fault hanging wall, new zealand, induced by distal south island earthquakes," *Geofluids*, vol. 15, pp. 216–239, 9 2014.